

**(Supporting Information)**

**Optically Active Poly(diphenylacetylene)s Showing Solvent-Dependent Helix Inversion  
Accompanied by Modulation of Helix Inversion Barriers**

Ravikumar Abilesh Kumar,<sup>a</sup> Tatsuya Nishimura,<sup>\*b</sup> Tsuyoshi Taniguchi,<sup>b,c§</sup> and Katsuhiro Maeda<sup>\*c</sup>

<sup>a</sup> Division of Nano Life Science, Graduate School of Frontier Science Initiative, Kanazawa University, Kakuma-machi, Kanazawa 920-1192, Japan

<sup>b</sup> Graduate School of Natural Science & Technology, Kanazawa University, Kakuma-machi, Kanazawa 920-1192, Japan

<sup>c</sup> WPI Nano Life Science Institute (WPI-NanoLSI), Kanazawa University, Kakuma-machi, Kanazawa 920-1192, Japan

\*To whom correspondence should be addressed. Email: nishimura@se.kanazawa-u.ac.jp,  
maeda@se.kanazawa-u.ac.jp

§ Present address: Interdisciplinary Research Center for Catalytic Chemistry, National Institute of Advanced Industrial Science and Technology (AIST), 1-1-1 Higashi, Tsukuba, Ibaraki 305-8565, Japan

## **Table of Contents**

- 1. Materials**
- 2. Instruments**
- 3. Synthesis of monomers**
- 4. Polymerization**
- 5. Determination of relative fluorescence quantum yield**
- 6. Helix inversion kinetics and barriers**
- 7. Supporting data**
- 8. References**
- 9. NMR spectral data**

## 1. Materials

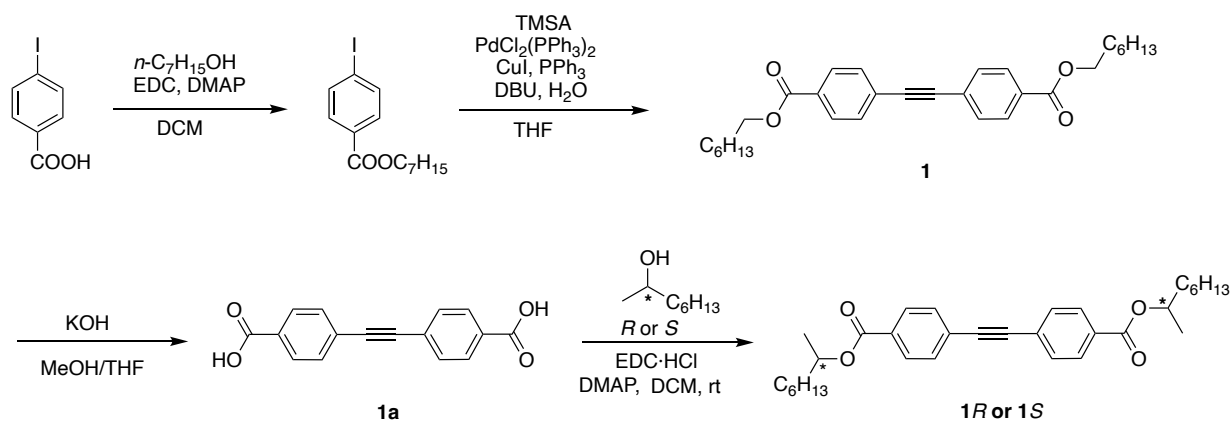
Commercially available reagents were used without further purification. Molybdenum pentachloride ( $\text{MoCl}_5$ ), *n*-heptanol, and potassium hydroxide (KOH) were purchased from FUJIFILM Wako pure chemical (Wako, Osaka Japan). Copper (I) iodide (CuI) and triphenylphosphine ( $\text{Ph}_3\text{P}$ ) were obtained from Kanto Kagaku (Tokyo, Japan) and Nacalai Tesque, Inc. (Kyoto, Japan), respectively. Tributylphenylstannane ( $\text{PhSn}^n\text{Bu}_3$ ) and bis(triphenylphosphine)palladium(II) dichloride ( $\text{Pd}(\text{PPh}_3)_2\text{Cl}_2$ ) were available from Sigma-Aldrich. (*R*)-(-)-2-octanol, (*S*)-(+)-2-octanol, *N,N*-dimethyl-4-aminopyridine (DMAP), 1,8-diazabicyclo[5.4.0]undec-7-ene (DBU), and 1-ethyl-3-(3-dimethylaminopropyl)-carbodiimide hydrochloride ( $\text{EDC}\cdot\text{HCl}$ ) were purchased from Tokyo Chemical Industry (TCI, Tokyo, Japan). Anhydrous tetrahydrofuran (THF), toluene, and dichloromethane (DCM) were purchased from Kanto Kagaku and were stored under nitrogen. Super dehydrated chloroform and ethyl acetate were available from Wako. Methylcyclohexane (MCH) and super dehydrated benzene were purchased from Kanto Kagaku. Chlorobenzene and *p*-xylene were obtained from TCI. Trimethylsilylacetylene (TMSA) was kindly supplied from Shinetsu Chemical (Tokyo, Japan). The monomer precursors **1**<sup>[S1]</sup> and **1a**<sup>[S2]</sup> were synthesized in a similar way to the reported method with slight modification (Scheme S1).

## 2. Instruments

NMR spectra were measured on a JNM-ECA 500 or JNM-ECZ 500 (JEOL) (500 MHz for  $^1\text{H}$  and 125 MHz for  $^{13}\text{C}$ ) spectrometer. IR spectra were recorded with a JASCO Fourier Transform IR-460 spectrophotometer. The size exclusion chromatography (SEC) measurements were performed with a JASCO PU-2080 liquid chromatograph equipped with a UV-vis (JASCO UV-970) detector at 40 °C using a Shodex (Tokyo, Japan) KF-805L SEC column. The temperature was controlled with a JASCO CO-1560 column oven. THF was used as the eluent at a flow rate of 1.0 mL/min. The molar mass calibration curves were obtained with polystyrene standards (Tosoh, Tokyo, Japan). Absorption and circular dichroism (CD) spectra were measured in a 1.0-mm quartz cell on a JASCO V-650 spectrophotometer and a JASCO J-725 spectropolarimeter, respectively. The temperature was controlled with a JASCO PTC-348WI apparatus. The concentration of polymers was calculated based on monomer units. The optical rotation was measured in a 10-cm cell at

25 °C on a JASCO P-2300 polarimeter. Dynamic light scattering (DLS) measurements were performed on a Zetasizer Nano ZSP (Malvern Panalytical, Worcestershire, UK) equipped with a 10 mW He-Ne laser (633 nm) at 25 °C. The polarizing optical microscope images were obtained from Olympus BX53 U-TP530 polarizer. Circularly polarized luminescence (CPL) spectra were obtained on a JASCO CPL-300 spectrofluoropolarimeter using a 1.0-cm quartz cell at room temperature. Elemental analysis was performed by the Research Institute for Instrumental Analysis of Advanced Science Research Center, Kanazawa University, Kanazawa, Japan.

### 3. Synthesis of monomers



**Scheme S1.** Synthesis of chiral monomers **1R** and **1S**

**Synthesis of di((*R*)-octan-2-yl)-4,4'-(ethyne-1,2-diyl)dibenzoate (**1R**).** To a solution of 4,4'-(ethyne-1,2-diyl)dibenzoic acid (**1a**) (5.0 g, 18.8 mmol), (*R*)-2-octanol (6.6 mL, 41.3 mmol), and DMAP (459 mg, 3.7 mmol) in anhydrous DCM (94 mL) was added EDC·HCl (12.5 g, 65.8 mmol) and the mixture was stirred at room temperature for 72 h. After dilution with DCM, the reaction mixture was washed with brine, and then dried over Na<sub>2</sub>SO<sub>4</sub>. The solvent was removed under reduced pressure and the crude product was purified by silica gel chromatography using *n*-hexane–ethyl acetate (95/5, v/v) as the eluent to give the desired product as a colorless viscous liquid (4.2 g, 48% yield).  $[\alpha]_D = -64.17$  (*c* 1.03, THF). IR (CaF<sub>2</sub>, cm<sup>-1</sup>): 1714 (C=O), 2218 (C≡C). <sup>1</sup>H NMR (500 MHz, CDCl<sub>3</sub>, 25 °C):  $\delta$  8.03 (d, *J* = 8.6 Hz, 4H), 7.59 (d, *J* = 6.9 Hz, 4H), 5.15 (m, 2H), 1.78–1.70 (m, 2H), 1.64–1.57 (m, 2H), 1.47–1.28 (m, 22H), 0.87 (t, *J* = 6.9 Hz, 6H). <sup>13</sup>C NMR (126 MHz, CDCl<sub>3</sub>, 25 °C):  $\delta$  165.7, 131.7, 130.8, 129.6, 127.2, 91.4, 72.2, 36.1, 31.8, 29.2, 25.5, 22.7,

20.2, 14.2. Anal. Calcd. for C<sub>32</sub>H<sub>42</sub>O<sub>4</sub>: C, 78.33; H, 8.63; N, 0.00. Found: C, 78.27; H, 8.55; N, 0.07.

The other chiral monomer **1S** was prepared in a similar way to the synthesis of **1R**. The details of spectroscopic data were given below,

**1S**: Colorless liquid, 48% yield. Spectroscopic data.  $[\alpha]_D = 63.18$  ( $c$  1.02, THF). IR (CaF<sub>2</sub>, cm<sup>-1</sup>): 1715 (C=O), 2217 (C≡C). <sup>1</sup>H NMR (500 MHz, CDCl<sub>3</sub>, 25 °C):  $\delta$  8.02 (d,  $J$  = 8.6 Hz, 4H), 7.59 (d,  $J$  = 8.6 Hz, 4H), 5.15 (m, 2H), 1.77-1.70 (m, 2H), 1.63-1.57 (m, 2H), 1.48-1.27 (m, 22H), 0.87 (t,  $J$  = 6.9 Hz, 6H). <sup>13</sup>C NMR (126 MHz, CDCl<sub>3</sub>, 25°C):  $\delta$  165.6, 131.6, 130.8, 129.6, 127.2, 91.4, 72.2, 36.1, 31.8, 29.2, 25.5, 22.7, 20.1, 14.2. Anal. Calcd. for C<sub>32</sub>H<sub>42</sub>O<sub>4</sub>: C, 78.33; H, 8.63; N, 0.00. Found: C, 77.92; H, 8.50; N, 0.18.

#### 4. Polymerization

Polymerization was carried out in a dry-sealed tube in toluene at 95 °C using the MoCl<sub>5</sub>-PhSn<sup>n</sup>Bu<sub>3</sub> catalytic system in a similar way as previously reported.<sup>[S3]</sup> The results of polymerization of **1R** and **1S** are summarized in Table S1.

**Table S1.** Polymerization results of **1R** and **1S** with MoCl<sub>5</sub>-PhSn<sup>n</sup>Bu<sub>3</sub> in toluene at 95 °C for 1 h<sup>[a]</sup>

Entry	Monomer	Polymer			
		Sample code	Yield% <sup>[b]</sup>	$M_n \times 10^{-5}$ <sup>[c]</sup>	$M_w/M_n$ <sup>[c]</sup>
1	<b>1R</b>	poly- <b>1R</b>	93	1.46	2.29
2	<b>1S</b>	poly- <b>1S</b>	94	1.68	2.21

[a] Monomer (0.41 mmol), MoCl<sub>5</sub> (0.02 mmol), PhSn<sup>n</sup>Bu<sub>3</sub> (0.02 mmol), toluene (0.41 mL).

[b] Methanol insoluble part. [c] Determined by SEC (polystyrene standards) with THF as eluent.

Spectroscopic data for poly-**1R**: IR (CaF<sub>2</sub>, cm<sup>-1</sup>): 1716 (C=O). <sup>1</sup>H NMR (500 MHz, CDCl<sub>3</sub>)  $\delta$  7.25-5.94 (br, 5H), 5.00 (br, 2H), 1.75-0.83 (br, 48H). <sup>13</sup>C NMR (126 MHz, CDCl<sub>3</sub>)  $\delta$  77.4, 77.1, 76.9, 31.9, 29.2, 22.7, 14.2 (aromatic carbons were unclear due to broadening).

Spectroscopic data for poly-1S: IR (CaF<sub>2</sub> cm<sup>-1</sup>): 1716 (C=O). <sup>1</sup>H NMR (500 MHz, CDCl<sub>3</sub>) δ 7.14-5.93 (br, 8H), 5.01 (br, 2H), 1.76-0.84 (br, 41H). <sup>13</sup>C NMR (126 MHz, CDCl<sub>3</sub>) δ 77.4, 77.1, 76.9, 31.9, 29.2, 22.7, 14.2 (aromatic carbons were unclear due to broadening).

## 5. Determination of relative fluorescence quantum yield

The relative fluorescence quantum yields ( $\Phi$ ) were calculated using the following equation:

$$\Phi_S = \Phi_R \times (A_R \times F_S \times \eta_S^2) / (A_S \times F_R \times \eta_R^2)$$

where  $A$  is the absorbance at the excitation wavelength,  $F$  is the area under the FL curve and  $\eta$  is the refractive index of the solvent ( $\eta = 1.33$  (H<sub>2</sub>O), 1.496 (toluene)). The subscripts  $S$  and  $R$  denote the respective values of the sample and reference substance, respectively. Quinine sulfate in sulfuric acid (0.1 mM) was used as the reference substance ( $\Phi_R = 0.55$ ,  $A_R = 1.155$ ,  $F_R = 490,015$ ), respectively. The concentration of sample and reference solutions was fixed at  $1.0 \times 10^{-6}$  mol/L in the measurement of the fluorescence spectra.

## 6. Helix inversion kinetics and barriers

### Theoretical formulae

From the initial slope of the changes in the ICD intensity in THF and toluene with time at different temperatures (30–60 °C), the pseudo-first order rate constants ( $k$ ) at 30, 40, 50, and 60 °C were estimated. The activation parameters for the helix inversion were estimated by the Arrhenius and Eyring plots according to the following equations:

$$\ln k = -(E_a/R) \cdot T^{-1} + b \quad (1)$$

$$\ln(k/T) = -(\Delta H^\ddagger / R) \cdot T^{-1} + \ln(k_B/h) + \Delta S^\ddagger / R \quad (2)$$

$$\Delta G^\ddagger = \Delta H^\ddagger - T \cdot \Delta S^\ddagger \quad (3)$$

where  $R$  is the gas constant (8.314 J·K<sup>-1</sup>·mol<sup>-1</sup>),  $k_B$  is the Boltzmann constant ( $1.381 \times 10^{-23}$  J·K<sup>-1</sup>), and  $h$  is the Planck's constant ( $6.626 \times 10^{-34}$  J·s<sup>-1</sup>).

### 6-1. Helix inversion kinetics and barriers of *M*-poly-1*R* to *P*-poly-1*R* in THF

The pseudo-first-order rate constants ( $k$ ) at 30, 40, 50, and 60 °C were estimated to be  $1.3 \times 10^{-5}$ ,  $5.2 \times 10^{-5}$ ,  $1.2 \times 10^{-4}$ , and  $3.5 \times 10^{-4}$ , respectively.

Using Eq.1, the activation energy ( $E_a$ ) was calculated (Figure S7 (b)).

$$E_a = 89.0 \text{ kJ/mol (21.3 kcal/mol)}$$

From Figure S7 (c),

$$\Delta H^\ddagger = 86.3 \text{ kJ/mol}$$

$$\Delta S^\ddagger = -53.1 \text{ J/(mol}\cdot\text{K)}$$

Using Eq. (3),

$$\Delta G^\ddagger = 86.5 \text{ kJ/mol (} T = 298 \text{ K)}$$

### 6-2. Helix inversion kinetics and barriers of *P*-poly-1*R* to *M*-poly-1*R* in toluene

Similarly to 5-1, helix inversion kinetics and barriers of *P*-poly-1*R* to *M*-poly-1*R* in toluene were calculated as described below.

The pseudo-first-order rate constants ( $k$ ) at 30, 40, 50, and 60 °C were estimated to be  $3.3 \times 10^{-6}$ ,  $1.8 \times 10^{-5}$ ,  $4 \times 10^{-5}$ , and  $2.8 \times 10^{-4}$ , respectively.

From Figure S8 (b),

$$E_a = 117.6 \text{ kJ/mol (28.1 kcal/mol)}$$

From Figure S8 (c),

$$\Delta H^\ddagger = 115.1 \text{ kJ/mol}$$

$$\Delta S^\ddagger = 29.5 \text{ J/(mol}\cdot\text{K)}$$

Using Eq. (3),

$$\Delta G^\ddagger = 115 \text{ kJ/mol (} T = 298 \text{ K)}$$

## 7. Supporting data

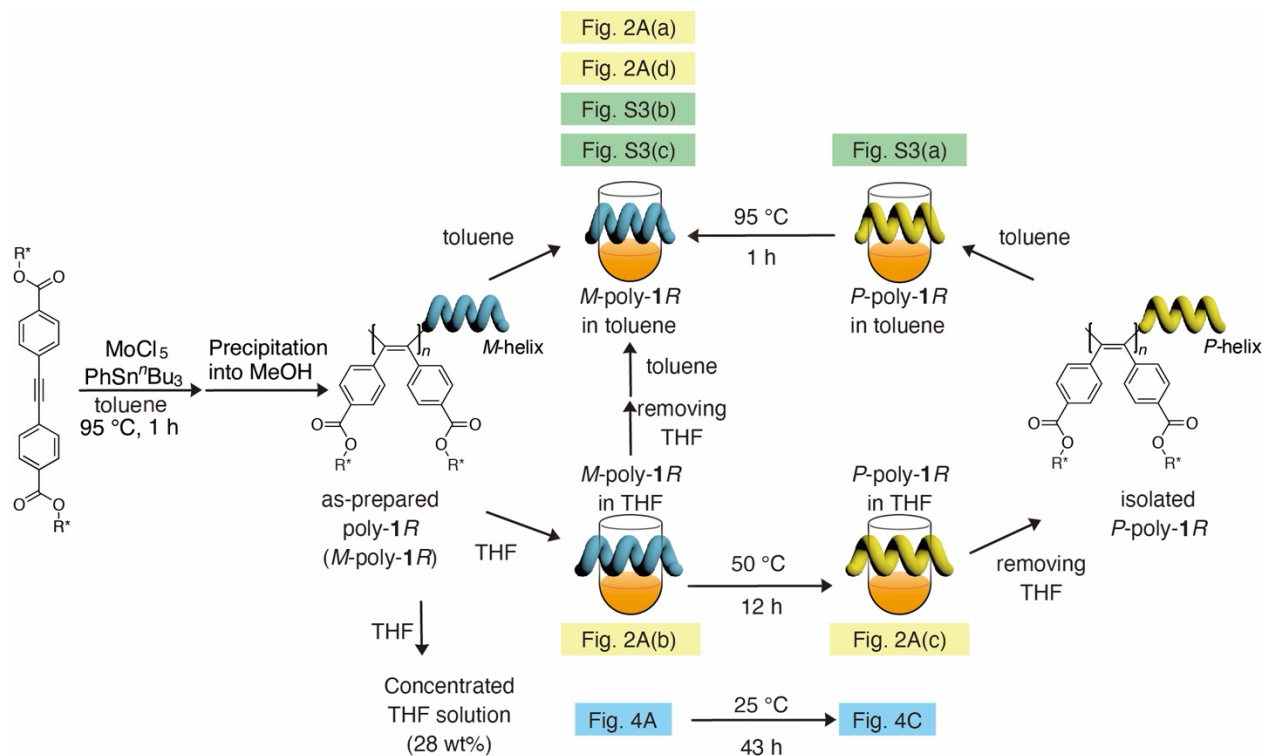


**Fig. S1.** Comprehensive procedural diagram for preparing *M*-poly-1R and *P*-poly-1R in respective solvents. The figure numbers corresponding to the spectral data are also shown. The LC sample was prepared by dissolving the as-prepared *M*-poly-1R in THF (28 wt%) and POM observation was carried out at 25 °C throughout the process.



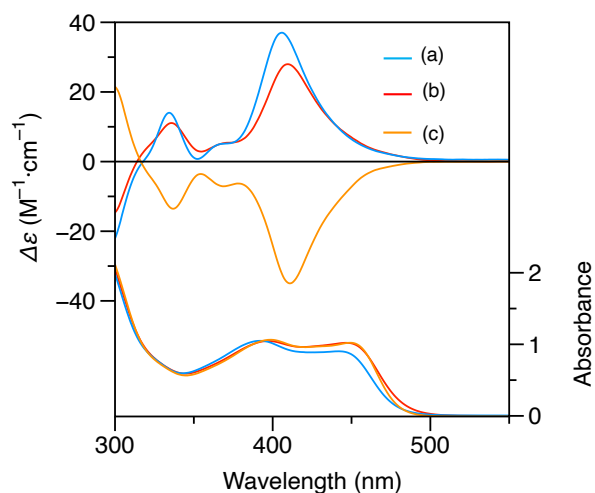


**Fig. S2.** CD and absorption spectra of poly-1S (1.8 mM) in toluene (a, blue line) and in THF before (b, red line) and after (c, orange line) thermal annealing at 50 °C for 12 h, measured at 25 °C.

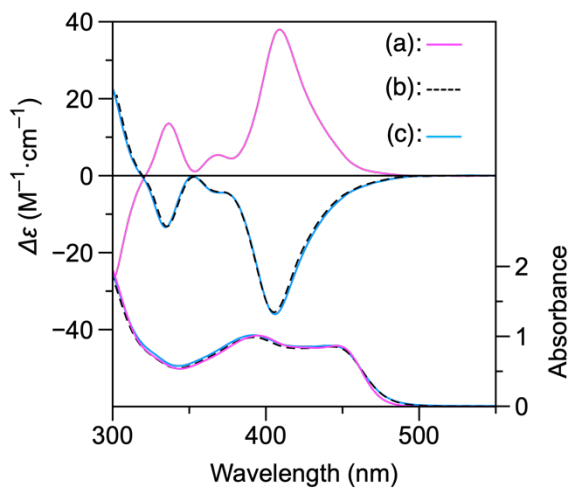


**Fig. S3.** (a) CD and absorption spectra of *P*-poly-1R (1.8 mM) prepared by thermal annealing at 50 °C for 12 h in THF, measured in toluene at 25 °C before (a, pink line) and after (b, dotted black line) thermal annealing at 95 °C in toluene for 1 h. (c) CD and absorption spectra of the as-prepared poly-1R measured in toluene at 25 °C (c, blue line).

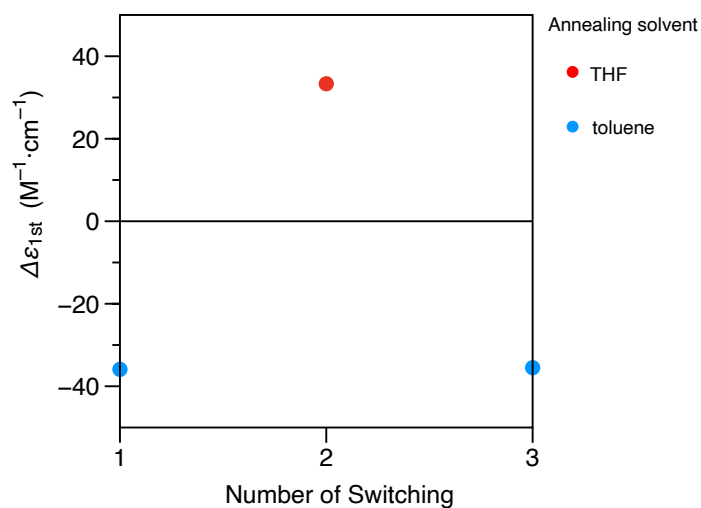


**Fig. S4.** Plots of CD intensity ( $\Delta\epsilon_{1st}$ ) of poly-1R (1.8 mM) after thermal annealing at 95 °C for 1 h in toluene (blue) and 50 °C for 12 h in THF (red), measured at 25 °C.

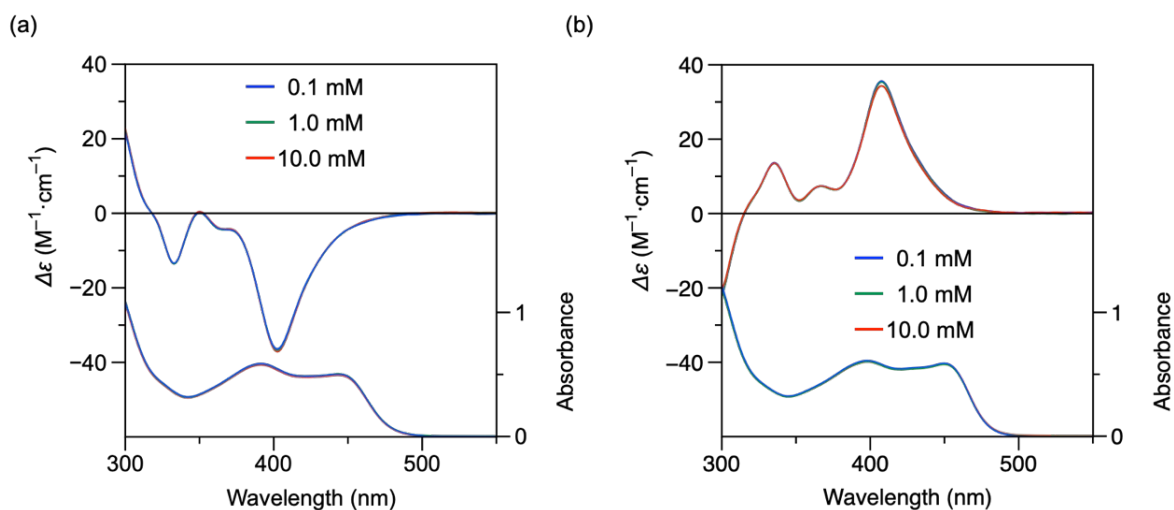


**Fig. S5.** CD and absorption spectra of  $M$ -poly-1R in toluene (a) and  $P$ -poly-1R in THF (b), measured at 25 °C at various polymer concentrations (0.1, 1.0, and 10 mM).

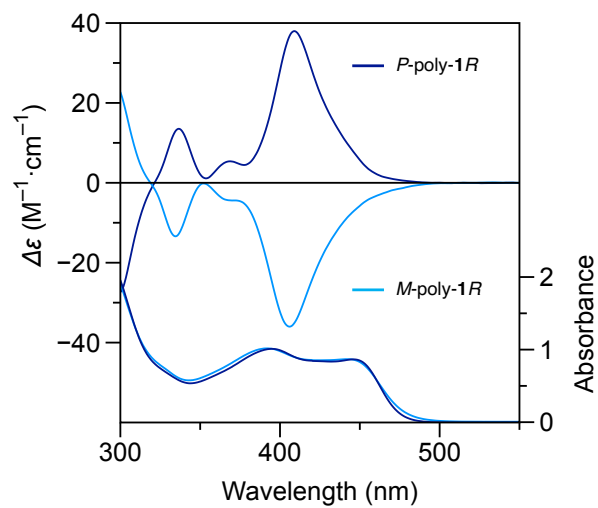


**Fig. S6.** CD and absorption spectra of  $M$ -poly-1R and  $P$ -poly-1R (1.8 mM) prepared by thermal annealing in toluene and THF, respectively, measured in toluene at 25 °C.

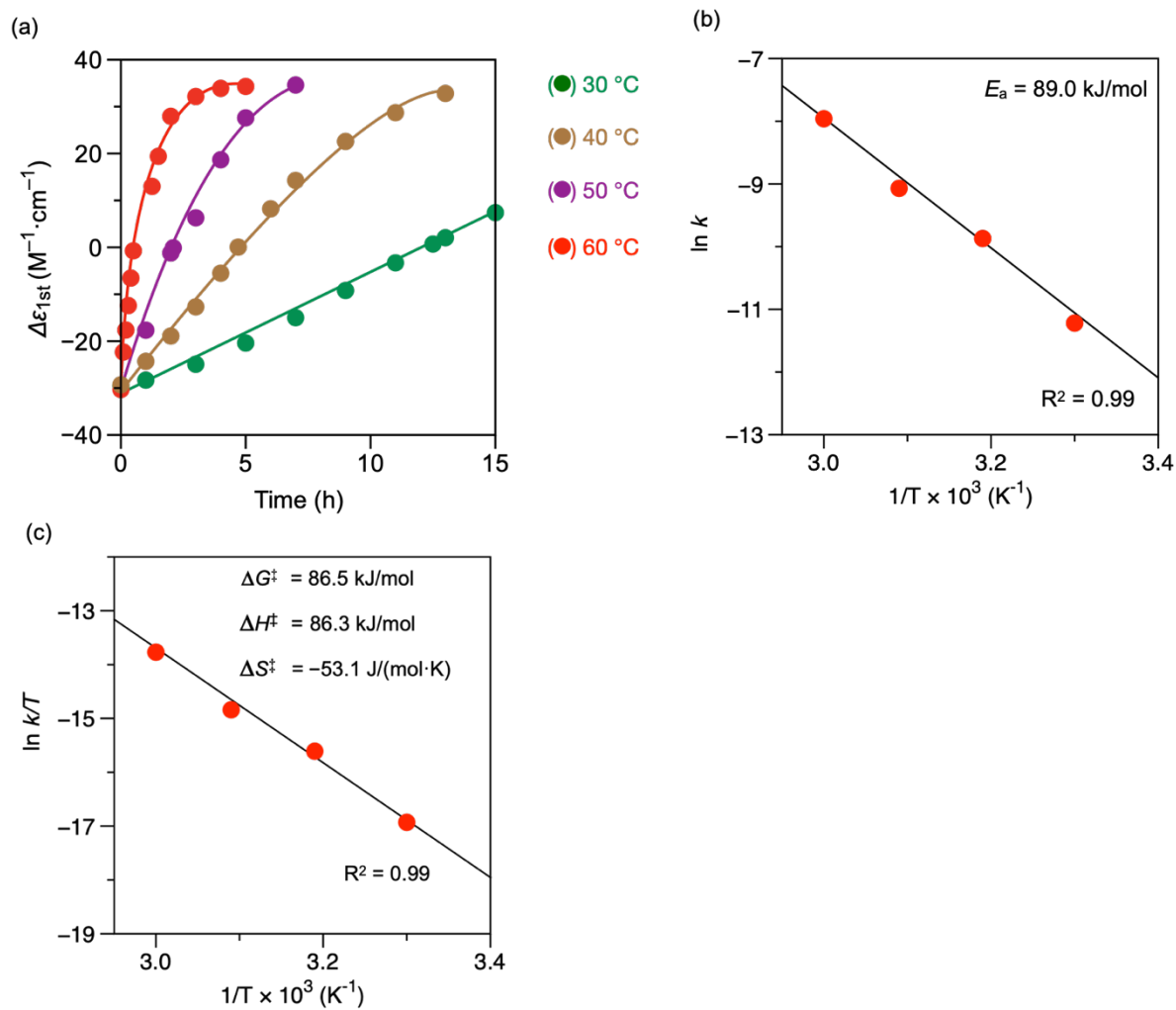


**Fig. S7.** (a) Time-dependent CD intensity changes of *M*-poly-1R to *P*-poly-1R in THF at various temperatures (30–60 °C). Arrhenius plots (b) and Eyring plots (c) of the temperature dependence of the pseudo-first-order rate constants obtained at 30–60 °C for *M*-poly-1R to *P*-poly-1R in THF. [polymer = 1.8 mM].

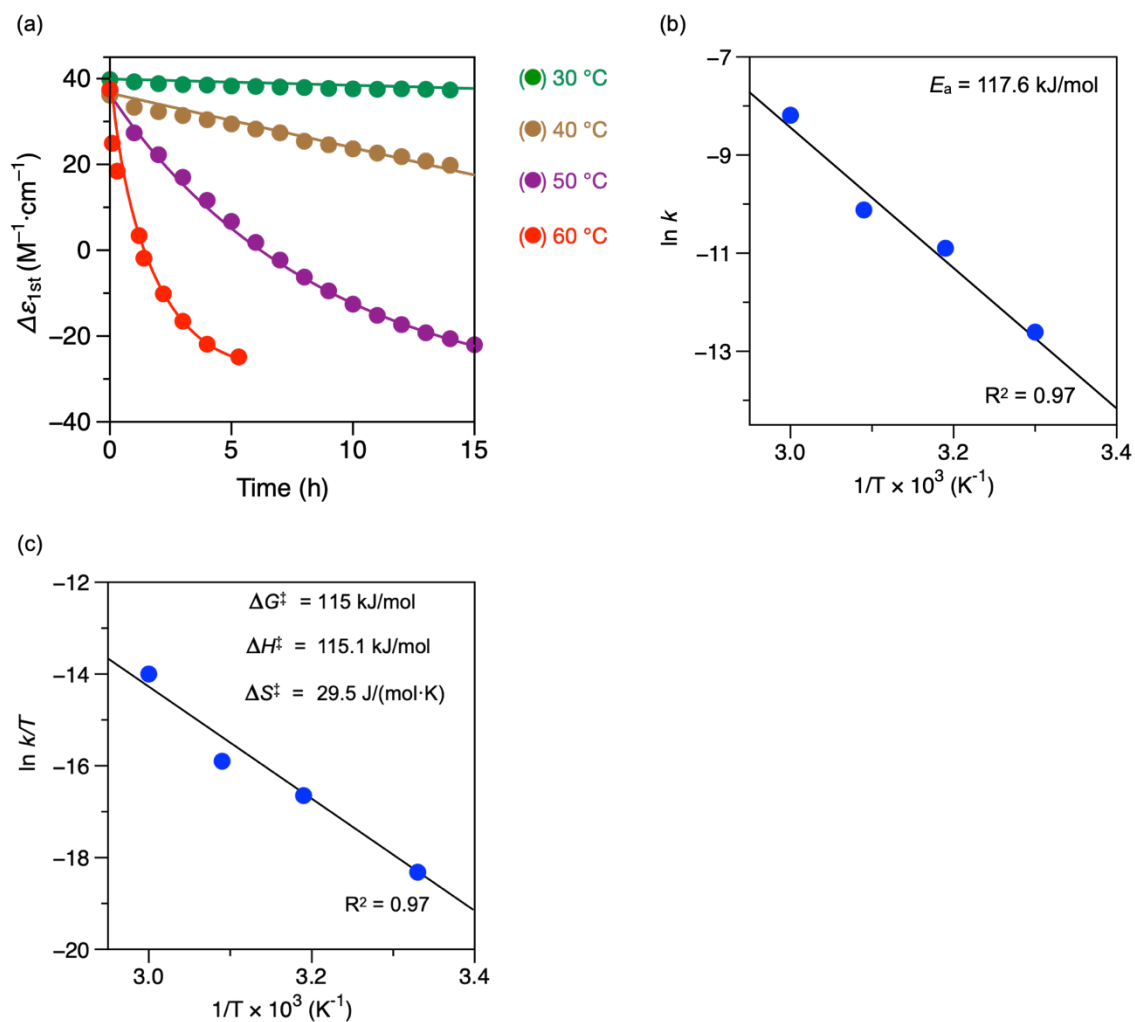


**Fig. S8.** (a) Time-dependent ICD intensity changes of *P*-poly-1*R* to *M*-poly-1*R* in toluene at various temperatures (30–60 °C). Arrhenius plots (b) and Eyring plots (c) of the temperature dependence of the first order rate constants obtained at 30–60 °C for *P*-poly-1*R* to *M*-poly-1*R* in toluene. [polymer = 1.8 mM].

## 8. References

- [S1] K. Maeda, M. Nozaki, K. Hashimoto, K. Shimomura, D. Hirose, T. Nishimura, G. Watanabe, E. Yashima, *J. Am. Chem. Soc.* **2020**, *142*, 7668-7682.
- [S2] T. Gadzikwa, B. Zeng, J. T. Hupp, S. T. Nguyen, *Chem. Commun.* **2008**, 3672–3674.
- [S3] M. Miyairi, T. Taniguchi, T. Nishimura, K. Maeda, *Angew. Chem. Int. Ed.* **2023**, *62*, e202302332.

## 9. NMR spectral data

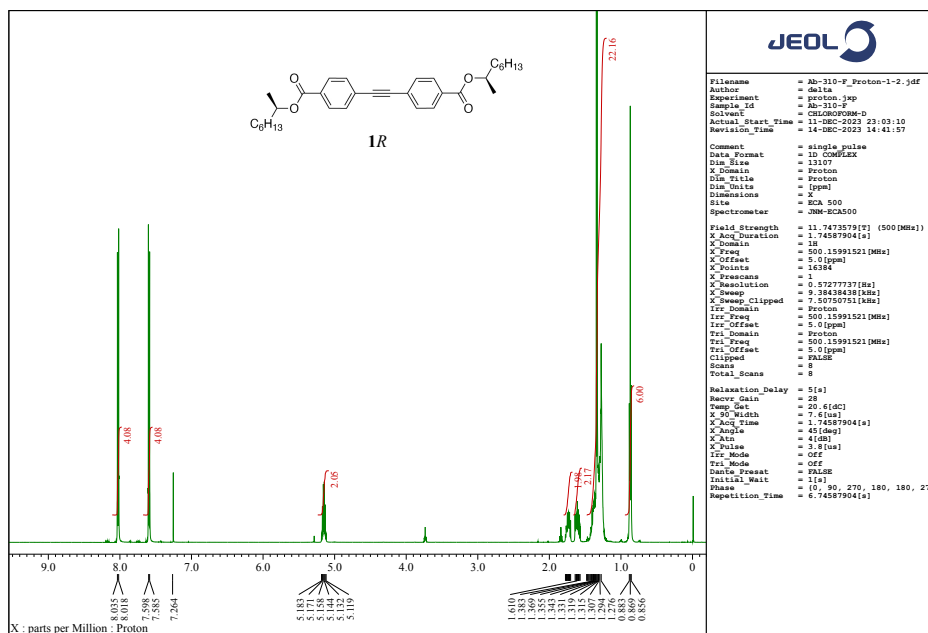


**Fig. S9.**  $^1\text{H}$  NMR (500 MHz,  $\text{CDCl}_3$ , 21  $^\circ\text{C}$ ) spectrum of **1R**.

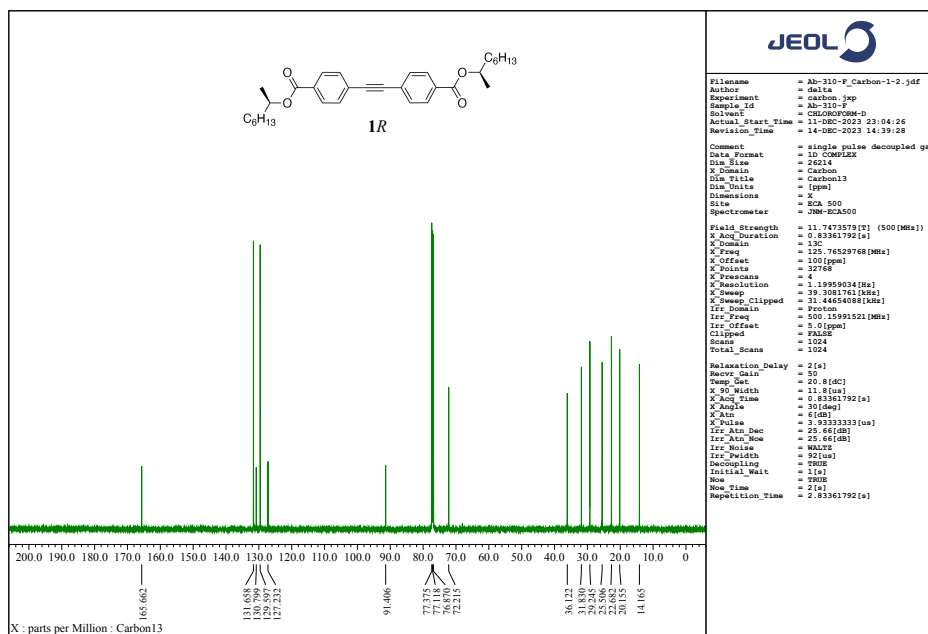


**Fig. S10.**  $^{13}\text{C}$  NMR (126 MHz,  $\text{CDCl}_3$ , 21  $^\circ\text{C}$ ) spectrum of **1R**.

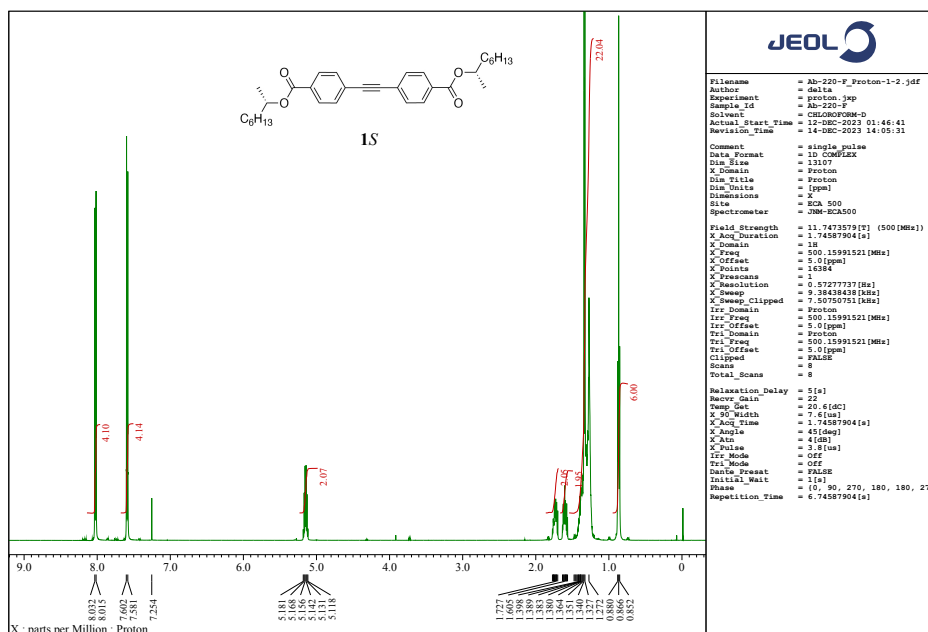


Fig. S11. <sup>1</sup>H NMR (500 MHz, CDCl<sub>3</sub>, 21 °C) spectrum of **1S**.

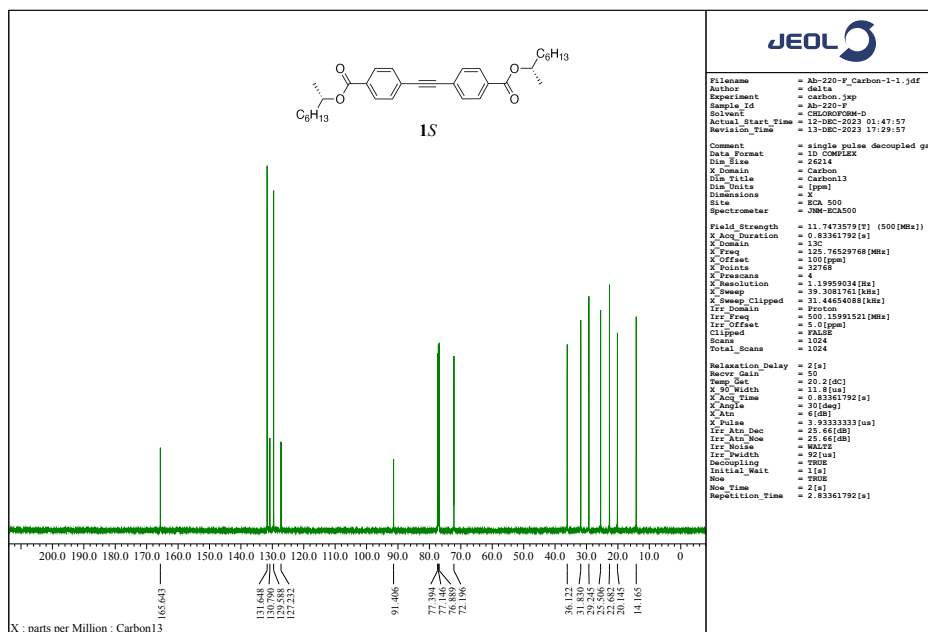


Fig. S12. <sup>13</sup>C NMR (126 MHz, CDCl<sub>3</sub>, 21 °C) spectrum of **1S**.



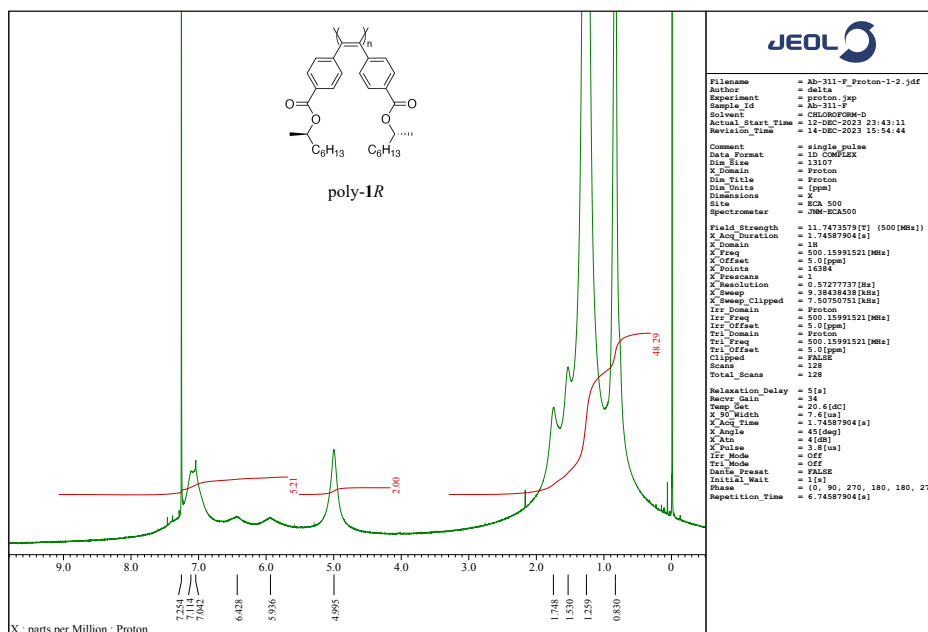


Fig. S13.  $^1\text{H}$  NMR (500 MHz,  $\text{CDCl}_3$ , 18  $^\circ\text{C}$ ) spectrum of poly-1R.

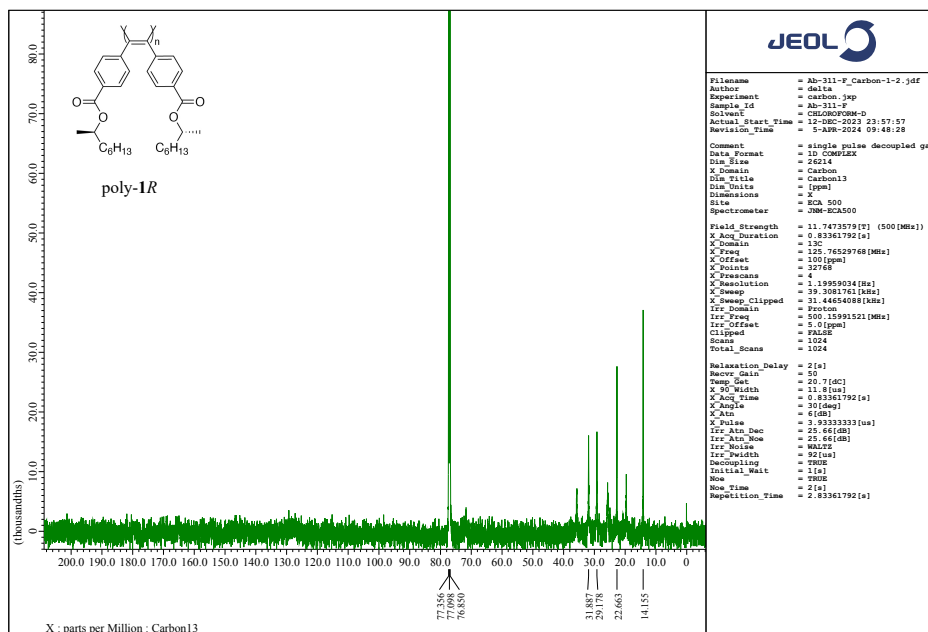
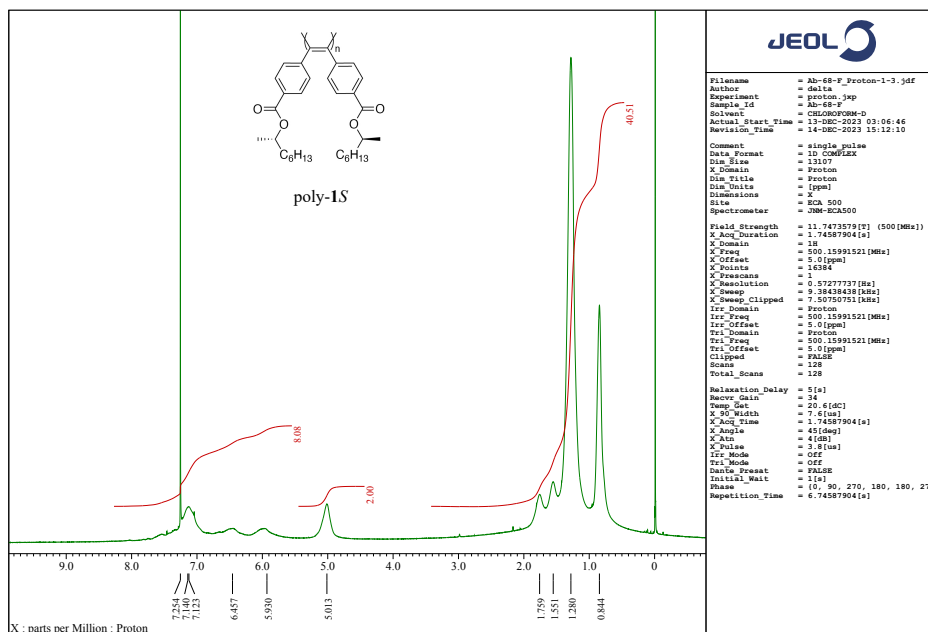
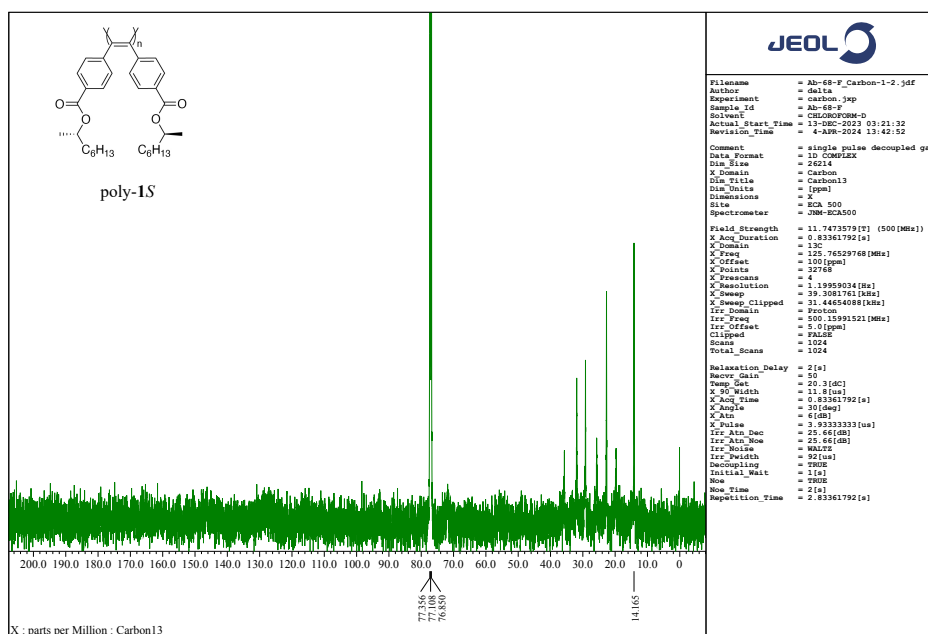


Fig. S14.  $^{13}\text{C}$  NMR (126 MHz,  $\text{CDCl}_3$ , 18  $^\circ\text{C}$ ) spectrum of poly-1R.



**Fig. S15.** <sup>1</sup>H NMR (500 MHz, CDCl<sub>3</sub>, 18 °C) spectrum of poly-1S.



**Fig. S16.** <sup>13</sup>C NMR (126 MHz, CDCl<sub>3</sub>, 18 °C) spectrum of poly-1S.